How to cite: *Angew. Chem. Int. Ed.* **2025**, *64*, e202419684
doi.org/10.1002/anie.202419684

Adhesive Polymers

Electrosynthesis of Mussel-inspired Adhesive Polymers as a Novel Class of Transient Enzyme Stabilizers

*Tilmann J. Neubert, Maximilian M. Hielscher, Keven Walter, Carolin M. Schröter, Marion Stage, Ruben R. Rosencrantz, Felix Panis, Annette Rompel, Kannan Balasubramanian, Siegfried R. Waldvogel, and Hans G. Börner**

In memory of Dr. Ehrhart Neubert

Abstract: Multifunctional ortho-quinones are required for the formation of thiol-catechol-connectivities (TCC) but can be delicate to handle. We present the electrochemical oxidation of the dipeptide DiDOPA, achieving up to 92 % conversion efficiency of the catechols to ortho-quinones. Graphite and stainless steel could be employed as cost-efficient electrodes. The electrochemical activation yields quinone-solutions, which are free of undesired reactive compounds and eliminates the challenging step of isolating the reactive quinones. The DiDOPA quinones were employed in polyaddition reactions with multi-thiols, forming oligomers that functioned as transient enzyme stabilizers (TES). These TCC-TES-additives improved the thermal stability and the activity of tyrosinase in heat stress assays.

The chemical industry is developing alternative pathways for common synthesis strategies to reduce energy consumption, install sustainable chemistry, and rethink resource management.[1] In this context, electrochemical and biocatalytic process strategies are often referred to as options to replace conventional chemical reactions, even at an industrial scale.[2] However, this requires efficient reactions based on affordable resources.[3] For example, for most transformations to selectively catalyze the desired reactions, electrosynthesis requires sustainable electrical energy, and inexpensive and non-consuming electrodes.[1a,2a,4] Similar prerequisites apply to biocatalytic reactions, where enzymes need to be available at adequate scale with robust activity to match technical processes. Among other factors, heat stress-induced denaturation, which triggers agglomeration and loss of enzyme activity, is a common challenges in biocatalysis.[2e,5] Engineering robust enzymes includes approaches like sequence evolution to improve structural stability, as well as synthetic enzyme modification, which primarily shields the enzyme from irreversible contacts that induces agglomeration.[6] Such a modification can be introduced either covalently to the protein periphery or non-covalently e.g. by soft hydrophobic interactions, hydrogen

[*] Dr. T. J. Neubert, K. Walter, C. M. Schröter, Prof. Dr. K. Balasubramanian, Prof. Dr. H. G. Börner
Humboldt-Universität zu Berlin
Department of Chemistry
Unter den Linden 6, 10117 Berlin (Germany)
E-mail: h.boerner@hu-berlin.de

Dr. T. J. Neubert, Prof. Dr. K. Balasubramanian
Humboldt-Universität zu Berlin
School of Analytical Sciences Adlershof (SALSA) & IRIS Adlershof
Unter den Linden 6, 10117 Berlin (Germany)

M. M. Hielscher, Prof. Dr. S. R. Waldvogel
Johannes Gutenberg University Mainz
Department of Chemistry
Duesbergweg 10–14, 55128 Mainz (Germany)

M. Stage, Prof. Dr. R. R. Rosencrantz
Fraunhofer Institute for Applied Polymer Research IAP
Life Science & Bioprocesses
Geiselbergstraße 69, 14476 Potsdam-Golm (Germany)

Prof. Dr. R. R. Rosencrantz
Brandenburg University of Technology BTU
Institute for Materials Chemistry, Chair of Biofunctional Polymermaterials
Universitätsplatz 1, 01968 Senftenberg (Germany)

Dr. F. Panis, Prof. Dr. A. Rompel
Universität Wien
Fakultät für Chemie, Institut für Biophysikalische Chemie
Josef-Holaubek-Platz 2, 1090 Wien (Austria)
Homepage: http://www.bpc.univie.ac.at

Prof. Dr. S. R. Waldvogel
Max-Planck-Institute for Chemical Energy Conversion
Stiftstraße 34–36, 45470 Mülheim an der Ruhr (Germany)

Prof. Dr. S. R. Waldvogel
Karlsruhe Institute of Technology (KIT)
Institute of Biological and Chemical Systems—Functional Molecular Systems (IBCS-FMS)
Kaiserstraße 12, 76131 Karlsruhe (Germany)

bonds, polyion-complexes or even specific peptidic contacts.[7]

Catechols and chemical derivatives are common motifs in a wide range of important natural small molecules as well as oligo- or polymers, ranging from dopamine to lignin, and acting for instance as signal transmitters, antioxidants, compatibilizers or adhesion promoters.[8] For materials science, the non-canonical amino acid L-dihydroxyphenylalanine (DOPA, Y*) has been of interest for decades as a potent interaction motif, which is found in e.g. mussel foot proteins and is the key residue for under-water adhesion.[9] DOPA is generated in vivo from tyrosine by monophenol oxidases.[9a,b,10] The adhesive strength of the catechol motif in DOPA has inspired a rich field of mussel-glue mimetic peptides and polymers, leading to adhesives with remarkable properties.[11]

Recently, a thiol-quinone Michael-type polyaddition mechanism has been established that leads to cysteinyldopa-inspired TCCs.[10a,12] These act as covalent linkers within the polymer chain and as points of potent non-covalent interactions. Chemically debondable pressure sensitive TCC-adhesives (PSA) could be realized using biscatechol A (BCA) or the dipeptide DiDOPA as TCC-building blocks.[12a] The DiDOPA-PSA showed improved potential for debonding applications in comparison to the BCA-variant, losing 99 % of its bonding strength upon oxidation. However, the more complex chemical structure of DiDOPA also rendered the development process more demanding. A prerequisite for TCC-polyaddition is the availability of multi-quinones, some of which like bisquinone A (BQA) can be readily isolated.[8a,11h,12e,f,13] However, DiDOPA quinone (BY*Q) undergoes unwanted side reactions during isolation, requiring an activation strategy for DiDOPA in solution, where BY*Q is stable.

Chemical activation using oxidation agents like sodium periodate ($NaIO_4$) or iodoxybenzoic acid (IBX)[14] seem to be straightforward. However, the required presence of the oxidation agent makes purification of BY*Q a resource intensive step that hampers scalability. The presence of the oxidation agents after activation leads to undesired side reactions such as disulfide formation in subsequent TCC-polyaddition reactions.[12a]

An alternative activation strategy is the use of enzymes like tyrosinase, which oxidizes tyrosine to DOPA and DOPA quinone in subsequent steps.[10c] While this is a valid strategy for monofunctional phenols and catechols,[10c] as well as peptides,[10a,12b,c,15] the conversion efficiency of multifunctional monomers is rather low. Furthermore, the simultaneous presence of quinones and catechols in water can lead to crosslinking and decay of the quinones.[12b,16]

Here, we explore electrosynthesis as an alternative pathway for the activation of multifunctional catechols represented by DiDOPA (Figure 1).[17] By electrochemical oxidation of DiDOPA to BY*Q, a solution containing only the reactive bisquinone is provided, which subsequently can be reacted with multi-thiols to form TCC-polymers. The strategy makes further purification steps obsolete, since organic solvents can be employed, which are stabilizing the bisquinone intermediates and support the TCC-formation reaction. First, the oxidative activation was optimized with low concentrations in batch-type cells to determine the best reaction conditions. Subsequently, these results were translated to flow cells and further optimized for higher throughput. The optimized conditions were used to create solutions containing BY*Q to react with various multi-thiols yielding a set of DiDOPA-TCC-oligomers (DY*-TCC). Based on the strong interaction capabilities of the DY*-TCC-segments, poly(ethylene glycol) (PEG)-based, water soluble TCC-oligomers were employed as transient enzyme stabilizers (TES) to protect the enzyme tyrosinase from heat stress. The TCC-TESs prevent thermal decay of the enzyme and increase their melting temperature by approx. 10 °C.

The electrochemical activation of DiDOPA to BY*Q and the subsequent thiol addition to form the TCC product were optimized by a series of experiments to identify the ideal combination of conditions for reaching a high conversion efficiency. Ethanethiol (EtSH) reacts as a model monothiol rapidly and selectively with quinones yielding $(EtSH)_n$-DY*-TCC compounds, with $n=1$ denoting a single addition and $n=2$ representing the desired two-fold addition product. The product mixture was analyzed by using liquid chromatography coupled with electrospray ionization mass spectrometry (LC–MS). The elugrams reveal the apparent conversion efficiency, which represents the fraction of catechol-groups converted to TCCs in relation to the total number of catechols (cf. Section 2 in Supporting Information—SI).

Depending on the conversion efficiency of the catechol activation process, the LC–MS elugrams contain fractions of unreacted DiDOPA, the single addition product with one ethanethiol and the two-fold addition product $(EtSH)_2$-DY*-TCC for full conversion (Figure S1). Overall, the TCC-formation between the quinone and the thiol is favored. Therefore, the ratio of the three species is indicative of the Faradaic efficiency of the electrochemical activation of the catechols in DiDOPA. The activation proceeds via the oxidation of both catechols independently, as they are chemically decoupled via the peptide backbone. Therefore, activation of just one catechol is possible, which is a common challenge for activation strategies of multifunctional monomers.[16,18] Alternative reaction pathways such as oxidative disulfide formation or oxidation transfer to TCC-catechols might reduce the electrochemically oxidized quinone back to the catechol form (Figure S2).[19] Consequently, those side reactions can diminish the overall conversion efficiency of catechol to TCC via the quinone. However, in the model reaction with a monothiol, a three-fold addition product was not detected in the LC–MS elugrams (Figure S3–S5). Therefore, it appears that the oxidation transfer pathway does not occur to a significant extent under the given reaction conditions.

First, DiDOPA was oxidized in small concentrations (5 mM) in batch-type cells varying different parameters like the solvent, the electrolyte, the anode and cathode material, as well as additives. The results are summarized in the Supporting Information (Section 2.1). All steps were optimized building upon each other, starting with platinum electrodes to identify the solvent and the supporting electro-

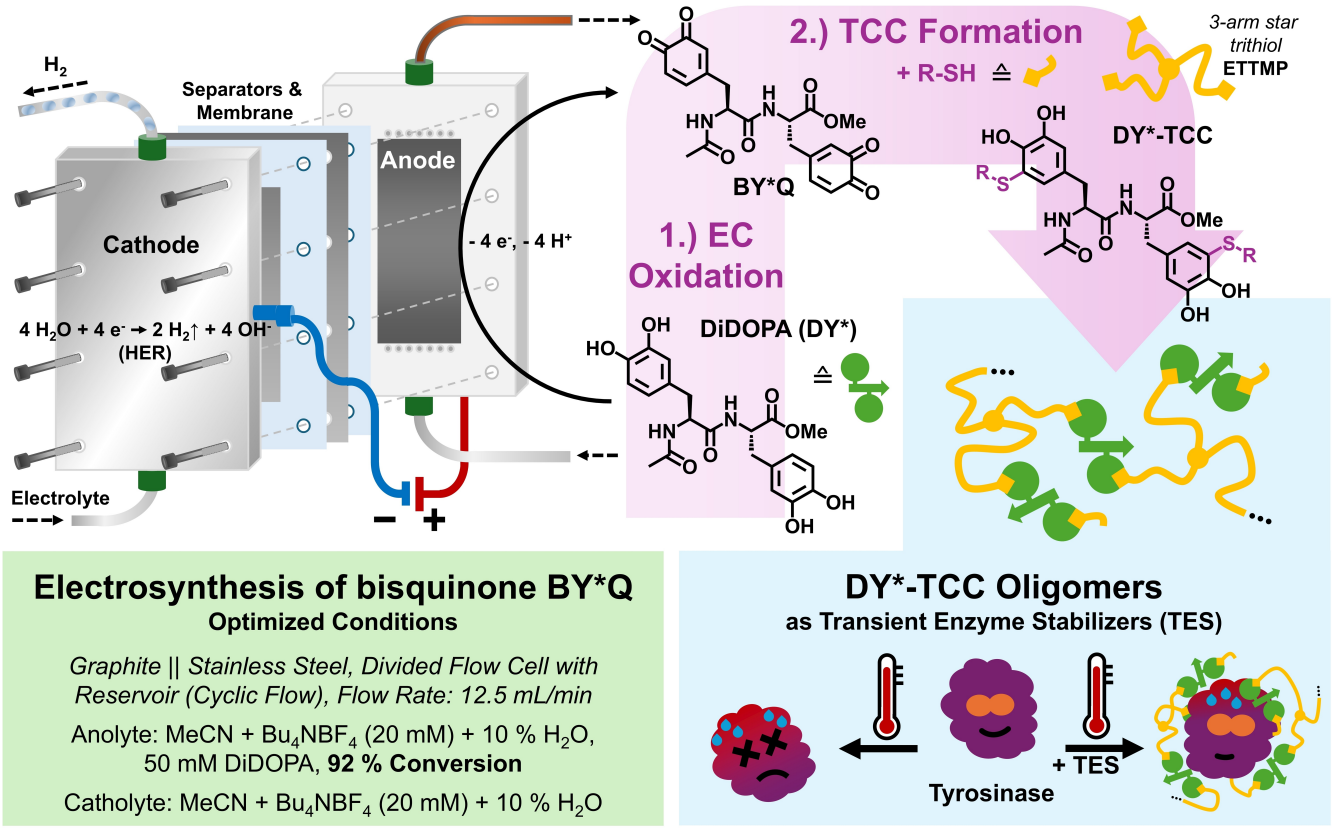

Figure 1. Electrosynthesis of TCC-oligomers via electrochemical oxidation of the biscatechol DiDOPA (DY*) to the corresponding bisquinone (BY*Q) with subsequent polyaddition via TCC-formation with multi-thiols. Due to the strong interaction motifs in DiDOPA, these oligomers can act as transient enzyme stabilizers to protect enzymes like tyrosinase from heat stress. The hydrogen evolution reaction (HER) is exploited as the cathodic half-cell reaction.

lyte. Therein, acetonitrile (MeCN) and tetrabutylammonium tetrafluoroborate (Bu_4NBF_4) were found to be the best choices for the electrolyte improving the conversion efficiency to 78 %, already (Table S1–S2). Subsequently, the anode and cathode were optimized, improving the conversion efficiency further to 84 % with isostatic graphite (Gr) as the anode and stainless steel (SS) as the cathode (Gr||SS, Table S3). Apart from the DiDOPA-oxidation at the anode, the half-cell reaction at the cathode also needs to be considered to avoid side reactions like solvent decomposition. This was achieved by promoting the hydrogen evolution reaction (HER).[20] Overall, Gr||SS consistently led to the best results in the batch-type cells, peaking at 92 % conversion efficiency for the activation and subsequent TCC-formation of DiDOPA, when used in MeCN with Bu_4NBF_4 and 10 vol.% water as an additive (Table S4).

To increase the reaction scale, a flow cell setup (2×6 cm^2 active surface per electrode) was employed. The initial screening rounds in this setup consistently yielded best results for the Gr||SS electrode combination, which was used for all follow-up studies. Conveniently, Gr||SS is also most promising for scale-up as these electrodes combine robustness with cost efficiency. Typically, a constant current of 5 mA/cm^2 (60 mA) was applied leading to a terminal cell voltage in the range of 2.7–3.5 V. The electrochemical activation is meant to provide a solution of BY*Q with a high concentration for the direct reaction with thiols and should be free of contaminants. Separating the half-cell reactions by a Nafion™ membrane proved to be advantageous for the efficiency and purity of the activated solution (Table S5). The concentration of DiDOPA was increased to 50 mM, which initially lowered the conversion efficiency to 32 % as compared to 44 % in case of 5 mM DiDOPA reaction solution (Table S6), suggesting that the Faradaic efficiency of the single pass setup was too low to reach satisfactory conversions. Increasing the amount of applied charge beyond the theoretically required four charge equivalents (4*F*) did not improve conversion sufficiently (Table S7). Therefore, the electrolyte feed was modified from single pass to a cyclic electrolysis with a stirred reservoir. In this setup, the conversion efficiency reached up to 88 % applying 6*F* to a 50 mM DiDOPA solution during the optimization (Table S8). Higher concentrations led to product precipitation and blockage of the outlet channel of the flow cell, which was detrimental for the process (Figure S6).

When the applied charge exceeded 6–7*F*, the apparent conversion efficiency decreased (Table S8). At the same time, a black precipitate formed on the electrode. At 12*F* this precipitate contaminated the solution severely (Fig-

ure S7). This could be attributed to overoxidation of the product that was accompanied by an increase in cell voltage to >4.5 V. The conversion efficiency decreases in these cases, as the residual DiDOPA is apparently not consumed, but the quinone product is lost due to the detrimental side product formation. The conversion efficiency neglects side reactions that form non-soluble products like this precipitate. After process optimization the resulting electrode passivation by the deposited coating could be mostly avoided by balancing maximized conversion of DiDOPA oxidation with minimized overoxidation and deposition. This compromise appears to be a drawback for the electrosynthesis route of quinones but might become interesting for some applications e.g. to access protective coatings. Under optimized conditions, the BY*Q activation with a pristine graphite electrode, gave quinone solutions that reacted with EtSH almost quantitatively to $(EtSH)_2$-DY*-TCC. The conversion efficiency of the overall reaction from catechol to TCC reached up to 92 % (Figure S8). The gravimetric isolated yield of the $(EtSH)_2$-DY*-TCC product was 64 %. The yield is lower than the apparent conversion efficiency due to side reactions.

As given in Figure 1 the optimized flow setup and activation conditions were used to prepare a solution of activated BY*Q, which was then reacted non-continuously with multi-thiols to form TCC-polymers via Michael-like thiol-quinone polyaddition reactions. Once the required amount of charge was passed, the activated bisquinone monomer solution was pumped out of the flow cell and multi-thiols were added in an assumed stoichiometry of 1:1. As previously proven, the thiol-quinone polyaddition reaction is generic, enabling use of several multi-thiols.[12a,e–h] These include the small dithiol 2,2'-(ethylenedioxy)-diethanethiol (EDET) to give linear TCC-polymers, as well as two PEG-based three-arm star trithiols (ETTMP) with molecular weights of M_n = 700 g/mol or 1300 g/mol and a poly(caprolactone)-based four-arm star tetrathiol (PCL4MP) with M_n = 1350 g/mol for branched TCC-polymers (Figure 2).

Size-exclusion gel permeation chromatography (GPC) analysis of the isolated products formed between the dithiol EDET and BY*Q, confirms the presence of the oligomeric TCC-polymerization product **EDET-DY*-TCC** (Figure 2). Matrix assisted laser desorption ionization time of flight mass spectrometry (MALDI-ToF-MS) revealed a homologous series of $(DiDOPA)_x(EDET)_y$ ($|x-y| \leq 1$) in a linear polymeric structure up to DP = 7 (Figure S9). The rather low degree of polymerization might result, on one hand, from low monomer concentration, as constrained by the electrochemical process parameters limiting DiDOPA concentration to 50 mM. On the other hand, the non-quantitative DiDOPA activation found in the electrochemical reaction step, leads to species with only one quinone that will partially terminate the AA + BB type step growth polyaddition.[12e] The accurate stoichiometry of reactive sites is of less importance in branched polyaddition reactions, e.g. bisquinone + tetrathiols. Therefore, GPC revealed for multi-thiols the formation of polymer products with broader molecular weight distributions, having high molecular

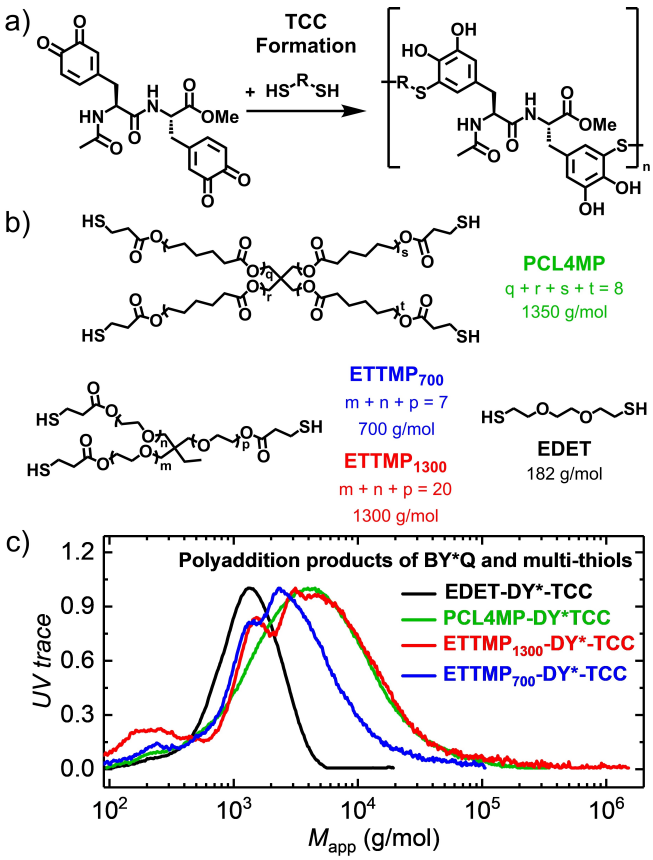

Figure 2. TCC-Polyaddition of BY*Q with multi-thiols. a) Idealized TCC-formation of DiDOPA (DY*) TCC-oligomers from electrochemically activated BY*Q with EDET. b) Structures of the multi-thiols used for TCC-polyaddition. c) Analysis of polyaddition products of electrochemically activated BY*Q and multi-thiols by gel permeation chromatography (GPC, polymerization conditions: 50 mM BY*Q in MeCN, thiol : quinone ≈ 1 : 1, RT, 3 h).

weight flanks that reach 60—100 kg/mol and suggesting branched topologies (Figure 2c, Table 1).

However, $M_{p,app.} < 5000$ g/mol confirms the formation of the desired TCC-oligomers fractions, as required for the targeted application as transient enzyme stabilizers. The chemical structures were confirmed by proton nuclear magnetic resonance (^{1}H NMR) and Fourier-transform infrared (FTIR) spectroscopy (SI-Section 3, Figure S10–S14). For the reaction of BY*Q with the branched trithiol macro-

Table 1: Key parameters extracted from GPC elugrams, including apparent number average ($M_{n,app.}$), weight average ($M_{w,app.}$) and peak ($M_{p,app.}$) molecular mass, the apparent degree of polymerization at the peak ($DP_{p,app.}$), and the polydispersity index ($Đ$). Polymerization conditions cf. Figure 2.

Oligomer	$M_{n,app.}$ [g/mol]	$M_{w,app.}$ [g/mol]	$M_{p,app.}$ [g/mol]	$DP_{p,app.}$	$Đ$
EDET-DY*-TCC	1100	1500	1400	2.3	1.3
$ETTMP_{700}$-DY*-TCC	2200	4100	2400	2.0	1.9
$ETTMP_{1300}$-DY*-TCC	3200	6500	3400	1.9	2.0
PCL4MP-DY*-TCC	2900	7200	4400	1.7	2.6

monomers, the respective monomers were found in an estimated ratio of 1.25:1 (DiDOPA:ETTMP$_{700}$) and 1.12:1 (DiDOPA:ETTMP$_{1300}$), implying that BY*Q and the ETTMP variants form a rather linear polymer with occasional crosslinks (about every fourth ETTMP-monomer). For the reaction of BY*Q with the tetrathiol PCL4MP, a ratio of 3.09:1 (DiDOPA:PCL4MP) was found, indicating a dense decoration of PCL4MP-thiols with DiDOPA linkers. The high ratio of DiDOPA to PCL4MP proves the superiority of the electrochemical approach to access BY*Q over chemical oxidation to avoid side reactions like disulfide formation.[12a] Using these estimated molecular ratios for the polymerization reactions a degree of polymerization (DP) could be roughly estimated from the $M_{p,app.}$ yielding $DP_{p,app.}$ in the range of 1.7–2.3 (Table 1).

Considering the high molecular weight flanks, a $DP_{app.}$ of up to 9 could be estimated for EDET-DY*-TCC, which is close to the DP = 7 found in MALDI-ToF-MS. As expected, the high molecular weight flanks of the traces of the branched DY*-TCC-products correspond to a higher $DP_{app.}$ of up to 30 for the product of ETTMP$_{700}$ and BY*Q (**ETTMP$_{700}$-DY*-TCC**) as well as the product of PCL4MP$_{1350}$ and BY*Q (**PCL4MP-DY*-TCC**) and up to 40 for the product of ETTMP$_{1300}$ and BY*Q (**ETTMP$_{1300}$-DY*-TCC**). The oligomers were isolated in a yield of up to 55 % (SI-Section 3).

The set of DY*-TCC-oligomer products has been targeted to be employed as transient enzyme stabilizers (TCC-TES). The oligomers combined branched polymer topologies comprising several TCC-adhesive sites and thus might be ideal to transiently "cage" and stabilize globular proteins as investigated on tyrosinase as a model enzyme. It is anticipated that the DY*-TCC-motifs, which feature catechol derivatives and peptidic backbones, will engage in robust interactions with the functionalities present at the surface of the enzyme. In combination with flexible segments of the star thiol monomers, which form loops between DY*-TCC-anchors, the formation of transient polymer/protein conjugation complexes might be expected. These dynamic decorations of the protein surface might inhibit protein-structure denaturation and improve the resistance against thermal stress.

As model enzyme the genetically expressed high-performance tyrosinase Sin(A)Tyr[10c] was investigated as monophenol-oxidase. The enzyme activity could be conveniently estimated using an established assay, which spectroscopically follows tyrosine oxidation to DOPA quinone in buffer solution.[12b,15a,21] Compatibility of the transient stabilizers with the enzyme and the activity assay requires water solubility of the DY*-TCC-oligomers, which is affected by the star-polymers. While both ETTMP variants contain PEG-segments that foster water solubility, the PCL4MP-based oligomer was too hydrophobic limiting water-solubility, as previously reported.[12a] Anyway, PEG proved to be highly suitable for protein/enzyme stabilization.[22] Non-covalent surface PEGylation with e.g. PEG-peptide conjugates has also been demonstrated to be an effective strategy for antifouling coatings.[23] Therefore, the effects of the ETTMP-DY*-TCC-oligomers (TCC-TES) on transient enzyme stabilization were investigated. Both ETTMP$_{700}$-DY*-TCC and ETTMP$_{1300}$-DY*-TCC were readily soluble in water and could be titrated with a solution of Sin(A)Tyr to constantly reach a TCC-TES/protein weight ratio of 1:1. The TCC-TES/enzyme complexes were allowed to equilibrate prior to nano differential scanning fluorimetry (nanoDSF) measurements to follow protein structure denaturation by temperature ramps from 25–95 °C at a rate of 1.5 °C/min. Figure 3a shows the denaturation curves for non-stabilized native Sin(A)Tyr in comparison to the TCC-TES-stabilized enzyme. The temperature of maximum denaturation rate ("melting" temperature T_m) shifted by approx. 10 °C, revealing that both TCC-TES additives seem to offset structural changes of the enzyme to elevated temperatures, which was confirmed to be stable for up to 50 days (Figure 3a–b, Figure S15, Table S9).

However, even more important than stabilizing the protein structure against thermal denaturation is the effect of the transient stabilizers on the enzymatic activity, which might be affected by mislocated "PEGylation", e.g. of the catalytically active pocket. A thermal stress activity assay was performed, where enzyme solutions have been heated to defined stress temperatures for 10 min and cooled down to room temperature to determine the residual enzyme activity (Figure 3c, Figure S16–17). The activity of the non-stabilized control was severely affected already after heating to 50 °C, while the TCC-TES-stabilized enzymes only lose their activity beyond 65 °C. Obvious stabilization effects were evident, when the activity of the stabilized Sin(A)Tyr in the presence of either TCC-TES additive was normalized to that of the non-stabilized control (Figure 3d). The activity after exposure to temperatures of 50–60 °C reached an increase of up to 250 % compared to the control (Figure 3d) and thus clearly confirms a protective effect of the TCC-TES additives. Remarkably, the enzyme activity in the presence of the TCC-TES additives was improved even at RT. Consistently, no activity was detectable after heating the enzyme to 80 °C in any case.

A few interesting effects were observed: In the presence of both TCC-TES additives, the Sin(A)Tyr shows a general trend to increased activity compared to the non-stabilized control. This positive influence of the additive might potentially be explained by minor changes in the dynamic protein structure, enabling faster substrate binding as described occasionally for PEGylated proteins.[24] Alternatively, the effect of increased enzyme activity might be linked potentially to allosteric activation or enzyme priming by the TCC catechols.[25] Moreover, the control shows reproducibly an atypically high activity at 65 °C, that drops back to the reduced level at 70 °C. This unusually high activity occurs at temperatures slightly above T_m of non-stabilized Sin(A)Tyr and might be linked to exposed active centers after unfolding of the enzyme. These observations support the hypothesis that the TCC-TES additives stabilize the enzyme by building-up a non-covalently attached periphery. It might be straightforward to speculate, that the well solvated, flexible PEG-chains of the star-polymer segments anchor temporarily via the TCC-DiDOPA adhesive sites to form transient complexes through interactions

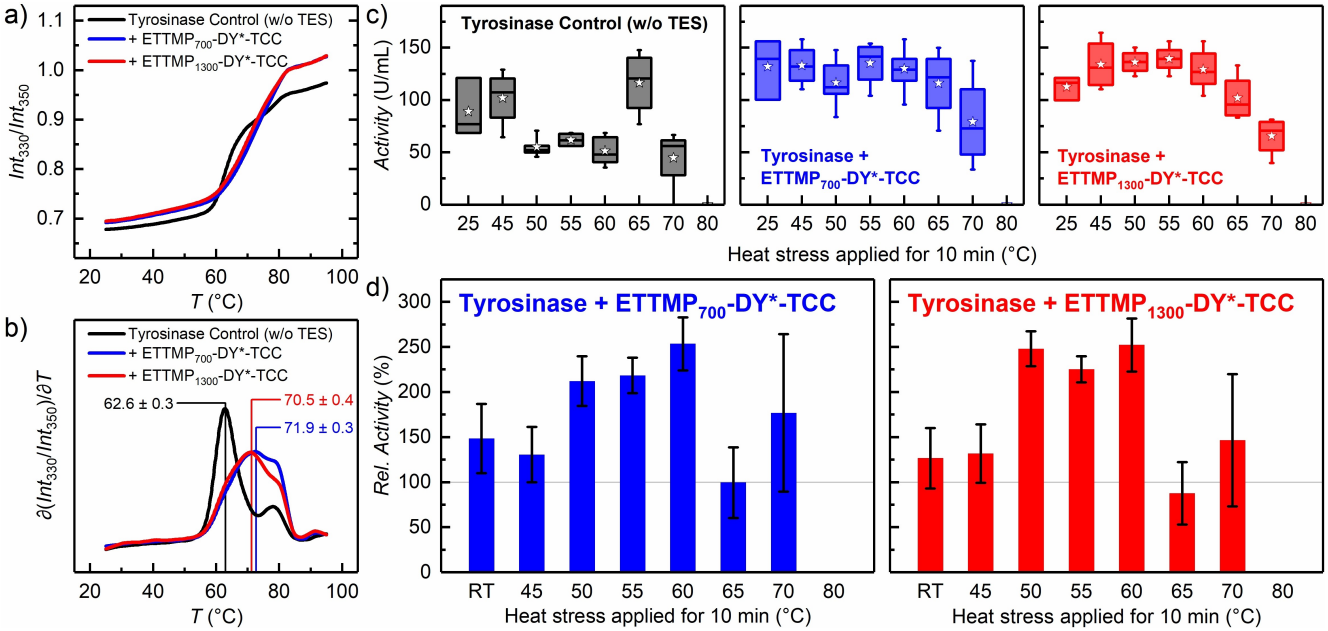

Figure 3. Thermal stability of tyrosinase Sin(A)Tyr in the presence of TCC-TESs. a) Thermal denaturation curves of Sin(A)Tyr with and without TCC-TESs determined by nanoDSF. b) First derivative of the curves in a) with T_m (mean of three independent measurements) indicated at the first maximum of each curve. c) Box plots of activity at room temperature of Sin(A)Tyr after exposure to heat stress at the indicated temperature for 10 min ($3 \leq n \leq 9$). d) Relative activity of Sin(A)Tyr in the presence of TCC-TESs normalized to the activity of control (w/o TCC-TES) after heat stress as indicated.

between TCC-catechols and functionalities present at the protein periphery. These complexes protect tyrosinase from heat stress, by counteracting thermally induced irreversible denaturation of the enzyme, preventing irreversible agglomeration and the loss of activity. Moreover, TCC-TES additives cause a general increase in enzyme activity even without prior thermal stress, as has been described for some covalently PEGylated enzymes.[24]

To elucidate the underlying stabilization effect, the enzyme solutions were subject to analysis using dynamic light scattering (DLS) in the absence and presence of the best performing TCC-TES additive ETTMP$_{700}$-DY*-TCC. In accordance with the concept of transient enzyme stabilization, DLS revealed that the average hydrodynamic radius (R_h) of the enzyme with or without TES remained unaffected in the range of 5 nm (Figure S18). This suggests that no permanent TES shell was formed around the enzyme, hinting at a very dynamic equilibrium that is shifted to the dissociated side at room temperature. This finding is consistent with the non-stressed enzyme activity data, showing no dramatic decrease at room temperature, but rather a slight increase of the enzyme activity. Apparently, the enzyme and the TCC-TES largely coexist in solution, and both retain their colloidal independence as there were no dramatic changes in the hydrodynamic particle sizes, even after exposure to heat stress up to 60 °C. However, consistent evidence of the stabilizing effect was provided by DLS, as in the presence of the TCC-TES the stabilized enzyme preserved its molecular dimensions after exposure to heat stress up to 70 °C, while the non-stabilized enzyme control agglomerated and precipitated out of solution. This suggests that the irreversible enzyme unfolding is prevented by the TCC-TES, avoiding agglomeration of the enzyme via e.g. emerging internal hydrophobic protein surfaces, while preserving dynamics to allow refolding when cooled to room temperature.

In conclusion, the electrochemical oxidation of multifunctional catechols to ortho-quinones has been demonstrated as a viable alternative to chemical approaches. For this process, graphite anodes and stainless-steel cathodes have been found as best electrode materials. The reaction was performed in an electrolyte consisting of acetonitrile and 10 vol.% water and Bu_4NBF_4 as supporting electrolyte in low concentrations. Therefore, the process is comparably inexpensive and more sustainable than approaches using oxidizers like periodate. In DiDOPA, both catechols were oxidized with high efficiency yielding solutions of DiDOPA quinone for the TCC-polyaddition to form oligomers with multifunctional thiols. Buffer-soluble variants of such TCC-oligomers showed promising properties as transient enzyme stabilizers, protecting the enzyme tyrosinase from activity loss upon heat stress. This catechol oxidation strategy is expected to be universally applicable. Furthermore, due to the variability of the backbone of the desired monomer, other polymers might be crafted via this strategy, allowing the use of electrosynthesis instead of conventional and waste-generating chemical agents.

Supporting Information

The data that support the findings of this study are available in the supplementary material of this article. (Materials and methods, detailed description and results of optimization of electrosynthesis, analytics, further details on tyrosinase assays.)

The authors have cited additional references within the Supporting Information.[26,27,28]

Acknowledgements

TJN, KW and HGB acknowledge funding by German Federal Ministry of Education and Research BMBF (IBZT-01 031B1117A) and German Science Foundation (DFG) BO 1762/15-1 (539647622) and BO 1762/9-2 (AOBJ 657247). TJN appreciates funding by the School for Analytical Sciences Adlershof (SALSA STF23-08). MMH thanks the German Science Foundation (DFG) for the opportunity to participate in the research training group GRK2516. The research was funded in part by the Austria Science Fund (FWF): 10.55776/P32326 to AR, 10.55776/P32932 to AR and ESP 10.55776/478-B to FP. Open Access funding enabled and organized by Projekt DEAL.

Conflict of Interest

The authors declare no conflict of interest.

Data Availability Statement

The data that support the findings of this study are available from the authors upon reasonable request.

Keywords: electrosynthesis · protein engineering · PEGylation · green chemistry · peptide adhesive

[1] a) D. S. Mallapragada, Y. Dvorkin, M. A. Modestino, D. V. Esposito, W. A. Smith, B.-M. Hodge, M. P. Harold, V. M. Donnelly, A. Nuz, C. Bloomquist, K. Baker, L. C. Grabow, Y. Yan, N. N. Rajput, R. L. Hartman, E. J. Biddinger, E. S. Aydil, A. D. Taylor, *Joule* **2023**, *7*, 23–41; b) J. Bremer, L.-M. Ränger, J. Friedland, *Nachr. Chem.* **2024**, *72*, 56–64.

[2] a) Y. H. Budnikova, E. L. Dolengovski, M. V. Tarasov, T. V. Gryaznova, *J. Solid State Electrochem.* **2024**, *28*, 659–676; b) R. Siedentop, T. Prenzel, S. R. Waldvogel, K. Rosenthal, S. Lütz, *ChemElectroChem* **2023**, *10*, e202300332; c) M. Zirbes, T. Graßl, R. Neuber, S. R. Waldvogel, *Angew. Chem. Int. Ed.* **2023**, *62*, e202219217; d) P. Moreno-García, M. d. J. Gálvez-Vázquez, T. Prenzel, J. Winter, L. Gálvez-Vázquez, P. Broekmann, S. R. Waldvogel, *Adv. Mater.* **2024**, *36*, 2307461; e) S. Wu, R. Snajdrova, J. C. Moore, K. Baldenius, U. T. Bornscheuer, *Angew. Chem. Int. Ed.* **2021**, *60*, 88–119; f) S. Zhang, J. Bramski, M. Tutus, J. Pietruszka, A. Böker, S. Reinicke, *ACS Appl. Mater. Interfaces* **2019**, *11*, 34441–34453; g) H. Chen, O. Simoska, K. Lim, M. Grattieri, M. Yuan, F. Dong, Y. S. Lee, K. Beaver, S. Weliwatte, E. M. Gaffney, S. D. Minteer, *Chem. Rev.* **2020**, *120*, 12903–12993; h) A. Wiebe, T. Gieshoff, S. Möhle, E. Rodrigo, M. Zirbes, S. R. Waldvogel, *Angew. Chem. Int. Ed.* **2018**, *57*, 5594–5619; i) J. Seidler, J. Strugatchi, T. Gärtner, S. R. Waldvogel, *MRS Energy Sustainability* **2021**, *7*, 42.

[3] M. Dörr, M. M. Hielscher, J. Proppe, S. R. Waldvogel, *ChemElectroChem* **2021**, *8*, 2621–2629.

[4] a) S. Arndt, D. Weis, K. Donsbach, S. R. Waldvogel, *Angew. Chem. Int. Ed.* **2020**, *59*, 8036–8041; b) S. B. Beil, D. Pollok, S. R. Waldvogel, *Angew. Chem. Int. Ed.* **2021**, *60*, 14750–14759.

[5] Q. Liu, G. Xun, Y. Feng, *Biotechnol. Adv.* **2019**, *37*, 530–537.

[6] a) I. Victorino da Silva Amatto, N. Gonsales da Rosa-Garzon, F. Antônio de Oliveira Simões, F. Santiago, N. Pereira da Silva Leite, J. Raspante Martins, H. Cabral, *Biotechnol. Appl. Biochem.* **2022**, *69*, 389–409; b) H. Wu, Q. Chen, W. Zhang, W. Mu, *Crit. Rev. Food Sci. Nutr.* **2023**, *63*, 2057–2073; c) C. Beaufils, H.-M. Man, A. de Poulpiquet, I. Mazurenko, E. Lojou, *Catalysts* **2021**, *11*, 497; d) P. V. Iyer, L. Ananthanarayan, *Process Biochemistry* **2008**, *43*, 1019–1032; e) C. Ó'Fágáin, *Enzyme Microb. Technol.* **2003**, *33*, 137–149.

[7] a) Y. Weng, S. Ranaweera, D. Zou, A. P. Cameron, X. Chen, H. Song, C.-X. Zhao, *Food Hydrocolloids* **2023**, *137*, 108385; b) F. S. Aalbers, M. J. Furst, S. Rovida, M. Trajkovic, J. R. Gomez Castellanos, S. Bartsch, A. Vogel, A. Mattevi, M. W. Fraaije, *eLife* **2020**, *9*, e54639; c) J. D. Brennan, D. Benjamin, E. DiBattista, M. D. Gulcev, *Chem. Mater.* **2003**, *15*, 737–745; d) D. Samuel, T. K. S. Kumar, G. Ganesh, G. Jayaraman, P.-W. Yang, M.-M. Chang, V. D. Trivedi, S.-L. Wang, K.-C. Hwang, D.-K. Chang, C. Yu, *Protein Sci.* **2000**, *9*, 344–352; e) N. S. Yadavalli, N. Borodinov, C. K. Choudhury, T. Quiñones-Ruiz, A. M. Laradji, S. Tu, I. K. Lednev, O. Kuksenok, I. Luzinov, S. Minko, *ACS Catal.* **2017**, *7*, 8675–8684.

[8] a) B. K. Ahn, *J. Am. Chem. Soc.* **2017**, *139*, 10166–10171; b) Z. Jia, M. Wen, Y. Cheng, Y. Zheng, *Adv. Funct. Mater.* **2021**, *31*, 2008821; c) J. Klein, K. Alt, S. R. Waldvogel, *Advanced Sustainable Systems* **2022**, *6*, 2100391; d) C. Zhang, L. Xiang, J. Zhang, C. Liu, Z. Wang, H. Zeng, Z.-K. Xu, *Chem. Sci.* **2022**, *13*, 1698–1705; e) A. Memarzia, M. R. Khazdair, S. Behrouz, Z. Gholamnezhad, M. Jafarnezhad, S. Saadat, M. H. Boskabady, *BioFactors* **2021**, *47*, 311–350; f) M. Bucciantini, M. Leri, P. Nardiello, F. Casamenti, M. Stefani, *Antioxidants* **2021**, *10*, 1044; g) Z. Yan, Y. Zhong, Y. Duan, Q. Chen, F. Li, *Animal Nutrition* **2020**, *6*, 115–123.

[9] a) S. Ito, T. Kato, K. Shinpo, K. Fujita, *Biochem. J.* **1984**, *222*, 407–411; b) T. J. Deming, *Curr. Opin. Chem. Biol.* **1999**, *3*, 100–105; c) J. H. Waiter, *Ann. N. Y. Acad. Sci.* **1999**, *875*, 301–309; d) H. Zhao, J. H. Waite, *Biochemistry* **2005**, *44*, 15915–15923; e) H. G. Silverman, F. F. Roberto, *Mar. Biotechnol.* **2007**, *9*, 661–681.

[10] a) J. Horsch, P. Wilke, M. Pretzler, M. Seuss, I. Melnyk, D. Remmler, A. Fery, A. Rompel, H. G. Börner, *Angew. Chem. Int. Ed.* **2018**, *57*, 15728–15732; b) H. Wagreich, J. M. Nelson, *J. Biol. Chem.* **1936**, *115*, 459–465; c) F. Panis, A. Rompel, *Environ. Sci. Technol.* **2023**, *57*, 13863–13873; d) S. C. Daubner, T. Le, S. Wang, *Arch. Biochem. Biophys.* **2011**, *508*, 1–12; e) S. H. Pomerantz, *J. Biol. Chem.* **1966**, *241*, 161–168.

[11] a) M. J. Harrington, A. Masic, N. Holten-Andersen, J. H. Waite, P. Fratzl, *Science* **2010**, *328*, 216–220; b) J. Yu, W. Wei, E. Danner, J. N. Israelachvili, J. H. Waite, *Adv. Mater.* **2011**, *23*, 2362–2366; c) H. Lee, N. F. Scherer, P. B. Messersmith, *Proc. Natl. Acad. Sci. USA* **2006**, *103*, 12999–13003; d) B. D. B. Tiu, P. Delparastan, M. R. Ney, M. Gerst, P. B. Messersmith, *ACS Appl. Mater. Interfaces* **2019**, *11*, 28296–28306; e) K. Lee, B. D. B. Tiu, V. Martchenko, K. Mai, G. Lee, M. Gerst, P. B. Messersmith, *ACS Appl. Mater. Interfaces* **2021**, *13*, 3161–3165; f) M. Cencer, Y. Liu, A. Winter, M. Murley, H. Meng, B. P. Lee, *Biomacromolecules* **2014**, *15*, 2861–2869; g) M. S. Ak-

ram Bhuiyan, J. D. Roland, B. Liu, M. Reaume, Z. Zhang, J. D. Kelley, B. P. Lee, *J. Am. Chem. Soc.* **2020**, *142*, 4631–4638; h) R. Pinnataip, B. P. Lee, *ACS Omega* **2021**, *6*, 5113–5118; i) C. R. Westerman, B. C. McGill, J. J. Wilker, *Nature* **2023**, *621*, 306–311; j) T. Christoff-Tempesta, R. M. O'Dea, T. H. Epps, III, *Macromolecules* **2023**, *56*, 9796–9803; k) G. Schmidt, K. H. Smith, L. J. Miles, C. K. Gettelfinger, J. A. Hawthorne, E. C. Fruzyna, J. J. Wilker, **2022**, *6*, 2100392; l) X. Li, Y. Zhang, G. Li, X. Zhao, Y. Wu, *Polymer* **2022**, *245*, 124693; m) G. D. Degen, P. Delparastan, B. D. B. Tiu, P. B. Messersmith, *ACS Appl. Mater. Interfaces* **2022**, *14*, 6212–6220; n) B. Cheng, J. Yu, T. Arisawa, K. Hayashi, J. J. Richardson, Y. Shibuta, H. Ejima, *Nat. Commun.* **2022**, *13*, 1892; o) J. Huang, Y. Liu, Y. Yang, Z. Zhou, J. Mao, T. Wu, J. Liu, Q. Cai, C. Peng, Y. Xu, B. Zeng, W. Luo, G. Chen, C. Yuan, L. Dai, *Science Robotics* **2021**, *6*, eabe1858; p) C.-Y. Lin, J. C. Liu, *ACS Applied Bio Materials* **2020**, *3*, 3894–3905; q) S. Chandna, C. A. Olivares M, E. Baranovskii, G. Engelmann, A. Böker, C. C. Tzschucke, R. Haag, *Angew. Chem. Int. Ed.* **2024**, *63*, e202313945.

[12] a) T. J. Neubert, K. Walter, C. Schroter, V. Guglielmotti, K. Hinrichs, S. Reinicke, A. Taden, K. Balasubramanian, H. G. Börner, *Angew. Chem. Int. Ed.* **2024**, *63*, e202408441; b) J. Horsch, P. Wilke, H. Stephanowitz, E. Krause, H. G. Börner, *ACS Macro Lett.* **2019**, *8*, 724–729; c) S. Arias, S. Amini, J. Horsch, M. Pretzler, A. Rompel, I. Melnyk, D. Sychev, A. Fery, H. G. Börner, *Angew. Chem. Int. Ed.* **2020**, *59*, 18495–18499; d) S. Arias, S. Amini, J. M. Krüger, L. D. Bangert, H. G. Börner, *Soft Matter* **2021**, *17*, 2028–2033; e) J. M. Krüger, H. G. Börner, *Angew. Chem. Int. Ed.* **2021**, *60*, 6408–6413; f) J. M. Krüger, C.-Y. Choi, F. Lossada, P. Wang, O. Löschke, D. Auhl, H. G. Börner, *Macromolecules* **2022**, *55*, 989–1002; g) C.-Y. Choi, F. Lossada, K. Walter, T. Fleck-Kunde, S. Behrens, T. Meinelt, J. Falkenhagen, M. Hiller, H. Oschkinat, A. Dallmann, A. Taden, H. G. Börner, *Green Chem.* **2024**, *26*, 2044–2058; h) C. M. Schröter, L. D. Bangert, H. G. Börner, *ACS Macro Lett.* **2024**, *13*, 440–445.

[13] a) G. D. Kang, K. H. Lee, C. S. Ki, Y. H. Park, *Fibers Polym.* **2004**, *5*, 234–238; b) M. Sugumaran, *Int. J. Mol. Sci.* **2016**, *17*, 1576; c) M. L. Alfieri, L. Panzella, S. L. Oscurato, M. Salvatore, R. Avolio, M. E. Errico, P. Maddalena, A. Napolitano, M. D'Ischia, *Biomimetics* **2018**, *3*, 26; d) Z. Jia, M. Wen, Y. Cheng, Y. Zheng, **2021**, *31*, 2008821.

[14] M. Frigerio, M. Santagostino, S. Sputore, *J. Org. Chem.* **1999**, *64*, 4537–4538.

[15] a) P. Wilke, H. G. Börner, *ACS Macro Lett.* **2012**, *1*, 871–875; b) P. Wilke, N. Helfricht, A. Mark, G. Papastavrou, D. Faivre, H. G. Börner, *J. Am. Chem. Soc.* **2014**, *136*, 12667–12674.

[16] M. Guazzaroni, M. Pasqualini, G. Botta, R. Saladino, *ChemCatChem* **2012**, *4*, 89–99.

[17] a) T. Kashiwagi, F. Amemiya, T. Fuchigami, M. Atobe, *Chem. Commun.* **2012**, *48*, 2806–2808; b) F. Sprang, S. R. Waldvogel, *ACS Electrochemistry* **2025**, *1*, 25–35.

[18] a) J. Meyers, N. Kurig, C. Gohlke, M. Valeske, S. Panitz, F. J. Holzhäuser, R. Palkovits, *ChemElectroChem* **2020**, *7*, 4873–4878; b) A. Wiebe, S. Lips, D. Schollmeyer, R. Franke, S. R. Waldvogel, *Angew. Chem. Int. Ed.* **2017**, *56*, 14727–14731; c) R. J.-R. Bednarz, P. Jiménez-Meneses, A. S. Gold, D. Monllor-Satoca, A. Stenglein, R. Gómez, S. R. Waldvogel, *ChemCatChem* **2023**, *15*, e202300606; d) R. J. R. Bednarz, A. S. Gold, J. Hammes, D. F. Rohrmann, S. Natalello, M. Mann, F. Weinelt, C. Brauer, S. R. Waldvogel, *Org. Process Res. Dev.* **2024**, *28*, 1529–1538.

[19] J. Mancebo-Aracil, C. Casagualda, M. Á. Moreno-Villaécija, F. Nador, J. García-Pardo, A. Franconetti-García, F. Busqué, R. Alibés, M. J. Esplandiu, D. Ruiz-Molina, J. Sedó-Vegara, *Chem. Eur. J.* **2019**, *25*, 12367–12379.

[20] M. Klein, S. R. Waldvogel, *Angew. Chem. Int. Ed.* **2022**, *61*, e202204140.

[21] H. W. Duckworth, J. E. Coleman, *J. Biol. Chem.* **1970**, *245*, 1613–1625.

[22] N. Nischan, C. P. R. Hackenberger, *J. Org. Chem.* **2014**, *79*, 10727–10733.

[23] S. Peplau, T. J. Neubert, K. Balasubramanian, J. Polleux, H. G. Börner, *Macromol. Rapid Commun.* **2023**, *44*, 2300300.

[24] N. Nischan, A. Chakrabarti, R. A. Serwa, P. H. M. Bovee-Geurts, R. Brock, C. P. R. Hackenberger, *Angew. Chem. Int. Ed.* **2013**, *52*, 11920–11924.

[25] C. J. Cooksey, P. J. Garratt, E. J. Land, S. Pavel, C. A. Ramsden, P. A. Riley, N. P. M. Smit, *J. Biol. Chem.* **1997**, *272*, 26226–26235.

[26] C. Gütz, B. Klöckner, S. R. Waldvogel, *Org. Process Res. Dev.* **2016**, *20*, 26–32.

[27] C. Gütz, A. Stenglein, S. R. Waldvogel, *Org. Process Res. Dev.* **2017**, *21*, 771–778.

[28] S.-H. Kim, K. Shin, B.-G. Kim, N. S. Hwang, T. Hyeon, *Chem. Commun.* **2023**, *59*, 94–97.

Version of record online: January 10, 2025